Journal of Chromatography, 517 (1990) 361–376
Elsevier Science Publishers B.V., Amsterdam

CHROMSYMP. 1940

Particle characterization in centrifugal fields

Comparison between ultracentrifugation and sedimentation field-flow fractionation

JIANMIN LI and KARIN D. CALDWELL*
Department of Bioengineering, University of Utah, Salt Lake City, UT 84112 (U.S.A.)
and
WALTER MÄCHTLE
Kunststofflaboratorium, BASF AG, D-6700 Ludwigshafen (F.R.G.)

ABSTRACT

A ten-component mixture of polystyrene latex particles in the 67–1220 nm size range was subjected to analysis by analytical ultracentrifugation (AUC) and sedimentation field-flow fractionation (SdFFF) using programmed and constant fields. The AUC analysis of the mixture yielded diameter values in good agreement with data determined on the separate components; the relative amounts of each component in the mixutre were likewise closely reproducing the sample's known composition. Diameters determined by SdFFF, either in a constant- or programmed-field mode, were in good agreement with the AUC for particles smaller than about 500 nm. For the sample's larger components, however, particularly the programmed mode showed diameter values smaller than expected. In addition, field programming resulted in incomplete recoveries of the larger particles, leading to more or less distorted mass distributions for the complex sample.

The observed discrepancies, which are thought to result from events at the analytical wall in the FFF channel, suggested a protocol for accurate sizing, as opposed to fingerprinting, of samples with broad size distribution. By tracking sizes and amounts of the different components at different but constant field strengths, and retaining as analytically valid only those data recorded in a retention range from five to about thirty column volumes, it was possible to determine sizes and amounts in good agreement with known parameters for the sample.

Unlike the AUC procedure, SdFFF produces fractions of a high degree of uniformity, which lend themselves to a secondary analysis, *e.g.* by electron microscopy, as shown in the study.

0021-9673/90/$03.50

INTRODUCTION

Since the days of Svedberg, centrifugal fields have been used routinely to determine sizes and size distributions for particulate samples in the diameter range 10–5000 nm[1]. Traditionally, such measurements are performed on dilute particle suspensions using the analytical ultracentrifuge, the optically transparent sample cell of which allows the operator to follow the unobstructed radial migration of a sample's components under the influence of the field. The rate of sedimentation at a given field strength is a measure of a spherical component's buoyant mass, which is convertible into an actual size if the densities of particle and suspension medium are known. Since amplitudes of the optical signals associated with each sedimenting species are measures of their relative amounts, the analytical ultracentrifugation (AUC) study leads to a determination of the sample's size distribution. Through the use of sensitive detection techniques[2–4] it is possible to perform the analysis at low sample concentration to avoid particle interactions and other non-ideal behavior. The technique is non-intrusive, and at the end of an analysis the sample can be retrieved for subsequent evaluation by other analytical methods. However, removing the field causes the components to remix, and any information relating size to, *e.g.*, composition or biological function, is not normally available by this route.

An alternate way of utilizing the field was proposed by Giddings, who in 1965 introduced the concept of field-flow fractionation (FFF)[5]. In the FFF mode of operation, the centrifugal field is applied perpendicularly to a laminar flow of suspension medium through a thin, flat channel. As in the ultracentrifugation experiment, particles injected into the FFF channel will migrate under the influence of the sedimentation field. However, their migration across the thin (typically 250 μm) channel is stopped by its outer wall where the particles are forced to accumulate and rapidly equilibrate. The field affects each particle in proportion to its mass, so that the more massive particles will form distributions that are more compact than those of lesser mass. Thus, a fully equilibrated polydisperse sample will consist of several exponentially distributed particle clouds superimposed on one another, each characterized by a thickness which relates to the mass of its constituents and to the strength of the applied field. This equilibration is normally allowed to occur with the liquid at rest, and as flow is resumed at the end of the relaxation period, the various particle zones are carried downstream with minimal disturbance of their equilibrium distributions. In the parabolic velocity profile maintained by the thin channel, zones of different degree of compression will move at different rates, so that the downstream transport results in a mass-based separation. At the end of the channel, the effluent is routed through one or more detectors, and the separated components may subsequently be collected for further analysis or evaluation.

The ability to fractionate polydisperse samples into cuts of a uniform and quantifyable particle size makes the FFF a powerful tool for particle characterization[6,7]. Ideally, the technique is applicable to samples ranging in size from a few tens of nanometers to well over a micrometer. An accurate sizing based on existing theory for so called "normal" FFF[8,9] requires that the particles behave as point masses, free from interactions with neighboring particles or with the accumulation wall. In practice, this condition may be difficult to meet for all components of a highly polydisperse sample. Often, the strong fields necessary to retain a distribution's finer particles to such

a degree that they can be accurately sized will force its large particles into extremely compact zones where steric effects[9] and overloading[10] lead to highly non-ideal behavior.

In the present study we make use of a ten-component mixture of nearly monodisperse polystyrene latex particles to compare performances of AUC and sedimentation FFF (SdFFF) in terms of accuracy in their diameter assignment as well as in their ability to determine relative amounts of each component. This comparison will demonstrate the overall good agreement between the two approaches for small particles. It will also pin-point some systematic errors encountered in the FFF analysis of particles larger than about 500 nm, and suggest operational procedures to reduce, or correct for, such errors, so that the positive features of the elution technique may be enjoyed even for samples of broad size distribution.

THEORY

Fig. 1 outlines the principal differences between AUC and SdFFF in terms of

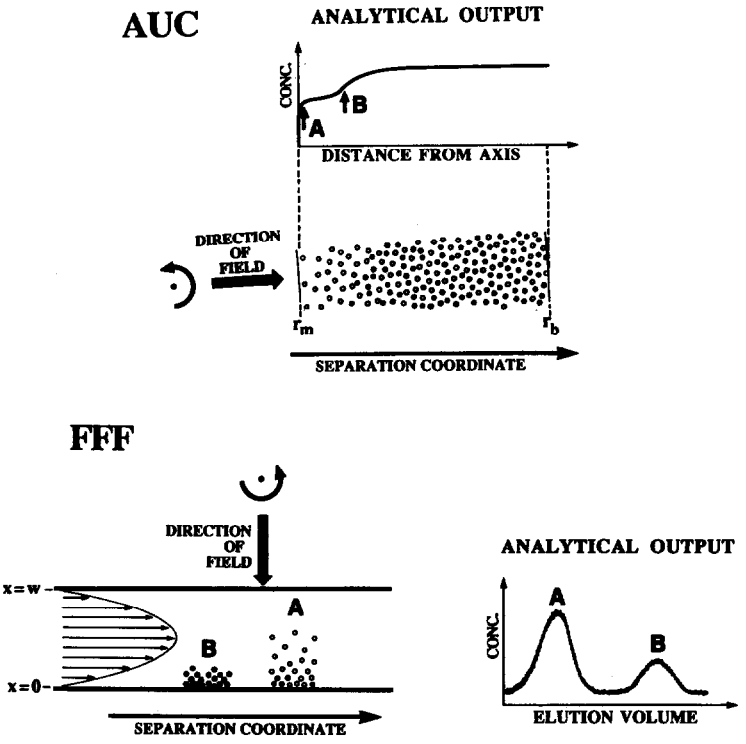

Fig. 1. Principles of AUC and FFF. The AUC analysis is based on the observation of rates of radial migration of the various depletion boundaries formed in the optically transparent analytical cell. Distances between the axis of rotation, the meniscus (r_m), and the outer wall (r_b) are not drawn to scale. The FFF analysis is based on the equilibrium distribution of sample in the thin (dimension w) separation chamber. Migration of the equilibrated sample constituents in a direction perpendicular to the field takes place at rates determined by the thickness of each sample zone. In both cases, solid black dots represent a more massive component than the open circles.

their use of the centrifugal field. In both applications, a particle of mass m and density ρ_s, which is suspended in a medium of density ρ, will experience a force F in the direction of the field. Under a gravitational acceleration G, the force is expressed by:

$$F = m(\Delta\rho/\rho_s)G \tag{1}$$

where $\Delta\rho$ is the density difference between particle and suspension medium. For spherical particles of diameter d, the mass m can be replaced by the product of volume and density:

$$F = (\pi d^3/6)\Delta\rho G \tag{2}$$

Stokes' law specifies the relationship between the particle's friction coefficient f, its diameter d, and the viscosity η of the medium:

$$f = 3\pi\eta d \tag{3}$$

which implies that the field induces the particle to move with a steady state velocity U, equal to:

$$U = F/f = d^2\Delta\rho G/18\eta \tag{4}$$

In AUC, this motion is quantified from observations of the movement of the various depletion boundaries which are created at the meniscus and transported outward towards the bottom of the cell. In evaluating d from the observed U, it is necessary to account for the fact that the boundary moves a significant fraction of the distance between the axis of rotation and the bottom of the cell[4], and that G therefore will vary with position r as measured from the axis:

$$G = \omega^2 r \tag{5}$$

Here, ω is the angular velocity of the rotor.

In FFF, the thin channel is positioned far enough from the axis of rotation that its thickness dimension w becomes a negligible fraction of r, and G therefore remains constant across the channel. Under the influence of the field, particles in the FFF channel will move radially, as in AUC. Due to the small gap width, their transport across the channel is rapid, and for particles denser than the medium accumulation takes place at the outer wall. After a brief relaxation period, the field induced concentration at the wall is exactly balanced by dispersion due to Brownian motion, and the particle zone is at equilibrium with a concentration distribution $c(x)$ in the direction of the field (x-axis), which is described by[8,11]:

$$c(x) = c(0)\exp(-x/\lambda w) \tag{6}$$

In this equation, λ is a dimensionless layer thickness related to the particles' drift velocity U and diffusivity D:

$$\lambda = D/Uw = kT/Fw \tag{7}$$

where k and T have the usual meaning of Boltzmann constant and temperature.

The concentration at the accumulation wall, expressed as $c(0)$ in eqn. 6, is rapidly increasing with decreasing λ; even for weakly retained samples, characterized by moderately large values of this parameter, $c(0)$ is well approximated by[10]:

$$c(0) = <c>/\lambda \tag{8}$$

where $<c>$ is the average sample concentration across the channel in the field direction.

Initiation of a laminar flow of liquid along the length dimension of the channel, *i.e.* in a direction perpendicular to the field, will transport the equilibrated particle zones downstream at rates determined by their respective λ values. Due to differences in zonal compression, resulting from differences in size and/or density, a mixture of particles will separate into its components during migration through the channel. The separated zones will emerge from the channel at different elution volumes V_e, which each bears a direct relationship to the characteristic layer thickness λ, and thus to the particle's diameter d (ref. 12) via eqns. 2 and 7:

$$V_0/V_e = R = 6\lambda[\coth(1/2\lambda) - 2\lambda] \tag{9}$$

The retention ratio R, defined as the ratio of average carrier velocity to sample velocity, is determined experimentally as the ratio of the channel's void volume V_0 to the elution volume V_e.

Eqn. 9 presumes the particles to be point masses, moving independently of one another without interactions with the wall. Larger particles become sterically excluded from the wall region, and corrections for this effect lead to a modified retention equation[13,14]:

$$R = 6\gamma(\alpha - \alpha^2) + 6\lambda(1 - 2\alpha)\{\coth[(1 - 2\alpha)/2\lambda] - 2\lambda/(1 - 2\alpha)\} \tag{10}$$

Here, α symbolizes $d/2w$, and γ is a factor the value of which appears close to unity. As will be discussed below, eqn. 10 fails to fully describe the retention of large particles, and attempts are presently under way to further modify the retention equation to correct for velocity and size dependent lift forces induced by the presence of the channel wall.

EXPERIMENTAL

Samples

The major focus of this study is a ten-component mixture of nearly monodisperse polystyrene (PS) latex spheres, prepared by BASF in the form of two nearly identical samples, referred to as "5" and "5R". The two mixtures are made up from the same close to monodisperse components, with the exception of the smallest particles which derive from different batches. The relative concentration of each component in these mixtures is 10% (w/w), and the density of the particles is reported to be 1.057 g/ml. In addition, the study uses monodisperse PS latex standards from Seragen.

Suspension medium (carrier)

For the AUC procedure, the medium is a 0.05% (w/v) solution of the ionic surfactant K30 (sodium salt of a [^{14}C]alkyl sulfonate from Bayer) in deionized water. In the case of SdFFF, the carrier is a 0.1% (v/v) solution in deionized water of the surfactant FL-70 from Fisher Scientific.

Equipment

The analytical ultracentrifuge at the Kunststofflaboratorium of BASF is an in-house modified version of a preparative ultracentrifuge (Model Omega 2) equipped with an analytical 8-cell rotor, both from Hereaus-Christ, which has been described in detail elsewhere[3]. Each 3-mm wide sector cell has a volume of 0.25 ml; the contents of all eight cells are monitored pseudo-continuously with a detection system based on the response by a photomultiplier to light traversing the cell, in a direction parallel to the axis of rotation, from a source emitting at 546 nm. An apertured mask with a 0.2-mm slit is positioned in the middle of each cell. The AUC detector response is corrected for Mie scattering, as described elsewhere[3,4], using $n(25°C, 546\ nm) = 1.59$ for polystyrene.

As the meniscus region becomes depleted with respect to particles of a given size, a concentration boundary is established the migration of which in the radial direction (across the perpendicular slit) can be followed as a function of time. The distance between meniscus and outer wall in these cells is kept constant at 1.30 cm, so that the distances between the axis of rotation and the meniscus, slit and outer wall are fixed at 5.85, 6.50 and 7.15 cm, respectively. Each cell is loaded with 0.25 ml of a 0.1% (w/v) sample suspension.

The SdFFF system was built at the University of Utah, essentially according to the description in ref. 15, although the rotor radius r in the present system is 15.5 cm, permitting the accommodation of a longer separation chamber; the dimensions of the present channel are 94 cm × 2.0 cm × 0.0254 cm for a measured void volume of 4.78 ml. The effluent from this system is monitored by a Linear Model 106 UV detector with a 254-nm light source, the output of which is fed to the system's IBM compatible AT personal computer. Elution volumes are based on weight, as described elsewhere[16], and are continuously input to the computer's RS232 port by the system's Ohaus Model C501 electronic balance. The field strength, relaxation time, and rate of carrier flow from the system's Minipuls 3 peristaltic pump Model 312, are all controlled by the computer. In the present study, sample volumes were 5 μl (1% solids), unless otherwise specified; the samples were manually injected at the head of the channel and allowed to relax for periods of 20 to 30 min. Absence of any effects of the length of the relaxation period on the level of retention was assured through multiple runs under different conditions. At the end of each run, diameters were evaluated from the elution position at peak maximum in accordance with eqns. 9 or 10, as specified by the operator. When needed, the detector response was corrected for Mie scattering as described in ref. 17, using 1.7685 (ref. 17) and 0.012 (ref. 18) as values for the real and imaginary parts of the refractive index for polystyrene, and 1.3702 as the real part of the refractive index for the carrier at 254 nm (the imaginary part being zero). The extinction cross sections calculated as described in ref. 17 were verified experimentally using polystyrene latex standards of accurately known concentrations. The area under each scattering corrected peak in the recorded fractogram was then found by integration after baseline

adjustment, and was considered proportional to the number of particles of the size determined from the peak elution volume; multiplication by the particle volume computed for this size gave the mass-based relative amount of the component.

The studies of recovery involved the observation fixed loads (4 μl of a sample suspension containing 1% solids) of standard polystyrene latices from Seragen. The areas under the elution peaks, recorded at different field strenths, were normalized by division with the area under a peak at no field. The small size of the void peak in fractograms collected at high particle retention obviated any correction for the presence of low-molecular-weight contaminants. As these studies involved comparisons of the behavior of one particle type at the time, there was no need to correct the detector response for Mie scattering.

Analysis of collected fractions

A BI-90 fixed-angle (90°) photon correlation spectrometry (PCS) system from Brookhaven Instruments was used routinely (in cases where the concentration of

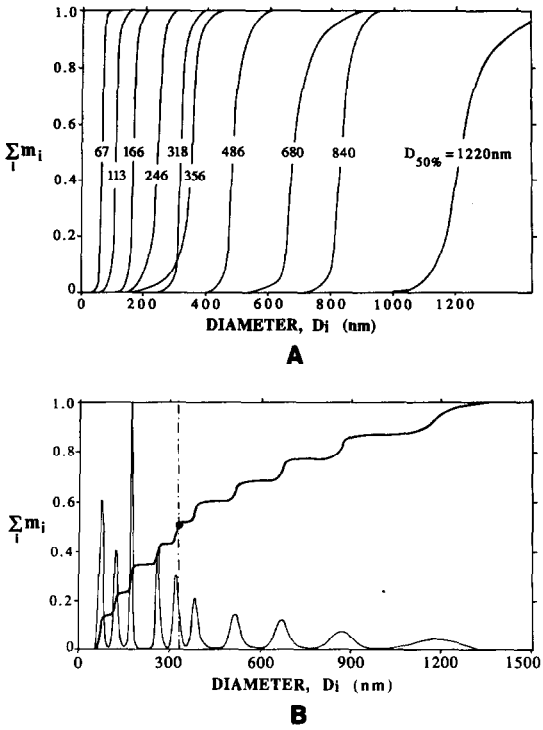

Fig. 2. (A) Size distribution curves for ten different polystyrene latex samples (density 1.057 g/ml) determined separately by AUC. The ordinate reflects the cumulative mass of particles below a given size D_i, indicated on the abscissa. (B) Size distribution curve for a mixture of the ten polystyrene latex samples analyzed separately in (A) (upper curve). Also shown (lower curve) is the derivative of the distribution function, the peak values of which indicate the average diameter for each component. The upper profile is a composite of two analyses run simultaneously in different cells, one at a sample concentration of 0.35 g/l (for the heavier components), and the other at 3.5 g/l. The heavy dot in the diagram represents the "coupling point"[4], indicating that data for larger diameters, D_i, derive from the lower concentration cell and smaller diameters from the higher.

TABLE I

PARTICLE DIAMETERS AND RELATIVE AMOUNTS DETERMINED FOR THE 10-COMPONENT MIXTURE OF PS LATEX PARTICLES USING DIFFERENT TECHNIQUES

Component No.	*Sample 5*		*Sample 5R*		*AUC-5*		*AUC-5R*		*DuPont*[a]		*SdFFF-C*[b]		*PCS*[d]*/SEM*[e]
	d(nm)	*%*	*d(nm)*	*%*	*d(nm)*	*%*	*d(nm)*	*%*	*d(nm)*	*%*	*d(nm)*	*%*	
1	67	10	85	10	85	12	72	14	70	26	96	—[c]	
2	113	10	116	10	116	10	121	9	119	16	113	8	
3	166	10	163	10	163	12	172	11	175	15	162	9	
4	246	10	257	10	257	11	259	8	261	13	259	16	252[d]/
5	318	10	306	10	306	10	320	10	319	11	320	18	307[d]/
6	356	10	365	10	365	11	379	8	374	9	376	17	381[d]/
7	486	10	504	10	504	9	515	9	479	7	524	10	/530[e]
8	680	10	650	10	650	6	665	8	588	3	716	9	/680[e]
9	840	10	834	10	834	9	870	10	695	0.5	917	7	/896[e]
10	1220	10	1142	10	1142	8	1180	13	805	0.5	1221	6	/1216[e]

[a] Data obtained from Dr. Roger Blaine of DuPont (published with permission). Analysis made in blind, using field programming in the time-delayed exponential mode.

[b] For an explanation of "SdFFF-C", see Results and Discussion section.

[c] The low resolution of this component from the void peak prohibits quantification.

[d] Diameters obtained by PCS.

[e] The magnification used in the SEM analysis of the FFF fractions does not allow accurate sizing of the smaller components. Relative amounts not obtained by this technique.

eluting particles was sufficient to permit a PCS analysis) to verify the diameters calculated from SdFFF.

Electron microscopy was performed on collected samples using a JEOL JFM 35 scanning electron microscopy (SEM) system. Prior to analysis, the collected fractions were concentrated on Nucleopore filters with pore sizes of 0.1 or 0.2 μm. The filtered samples were mounted on copper stubs and gold coated prior to imaging.

RESULTS AND DISCUSSION

AUC of each of the ten polystyrene latices prepared by BASF yields the size distributions shown in Fig. 2A; particle diameters reported in Table I as "Sample 5", and "Sample 5R", respectively, are determined from the midpoints of such distribution curves. Fig. 2B shows the result of an AUC analysis of that mixture of the ten components, referred to as "Sample 5". In order to produce this distribution curve, the rotor was ramped up during the 1.5-h run in an essentially exponential fashion[4], from 0 rpm via weak fields suitable for generating readily measurable sedimentation velocities for the largest particles in the mixture, to a final spin rate of 40 000 rpm. The sizes determined for each constituent in the AUC analysis of the two sample mixtures are listed as AUC 5 and AUC 5R in Table I. The duration of these runs ranged from 1 to 2 h. As is seen from this table, the AUC is faithfully reproducing both the number of components in the mixture as well as their sizes and relative amounts.

In contrast to the AUC analysis just described, field-programmed SdFFF begins at a high spin rate, which produces retention even of small particles, and progresses to weaker fields where, ideally, the more massive particles are being transported through the channel at measurable rates[19]. Fig. 3 represents a 4-h SdFFF run of the sample using the time-delayed exponential program introduced by Yau and Kirkland[20]. The experimental parameters chosen to produce Fig. 3 were not optimized for high resolution; yet, the run is clearly informative as to the complexity of the sample. The presence of at least nine components is indicated, and the tenth could presumably have been resolved, had we been able to spin our system at a higher speed than the 2000 rpm (692 g) which is our current upper limit.

The ten-component sample (Sample 5) was also submitted for a routine analysis (analytical conditions not optimized) to DuPont, whose SF[3] Particle Fractionator was

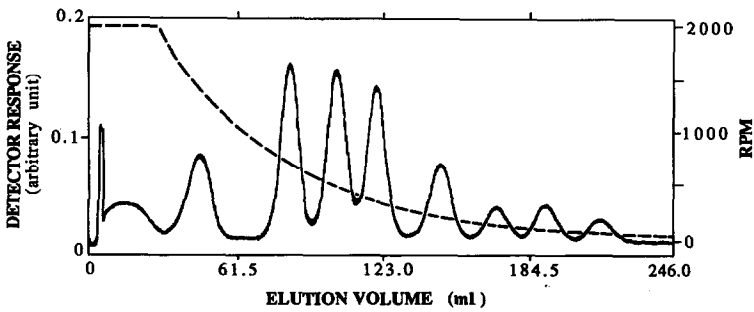

Fig. 3. Screening of the ten-component polystyrene latex sample, using field-programmed SdFFF. The form of the program was a time-delayed exponential, with an initial field of 2000 rpm and a time constant of 20 min: the flow-rate was 1.0 ml/min.

the first SdFFF instrument to be produced commercially. In contrast to the Utah system, DuPont's SF[3] is capable of handling spin rates of 18 000 rpm (35 000 *g*), and could therefore resolve and quantify even the smallest particles of the mixture, as seen in Table I; the duration of this analysis was around an hour. Although diameter assignments for the smaller particles (less than 500 nm) were in good agreement with the AUC data, the table shows an increasing departure from the nominal diameter values with an increase in size. From Table I it is also clear that quantification of the larger components is less accurate, as recoveries appear to decrease with increasing particle size.

As seen from eqn. 8 above, the exponential distribution of sample in the field direction implies a concentration at the accumulation wall which is inversely related to λ. Since λ, in turn, is an inverse function of the product d^3G, it follows that an increase in G has a strongly compressing effect, particularly on zones containing large particles; hence, any tendency of the particles to adsorb at the solid–liquid interface will be promoted by increased wall concentrations, *i.e.* by increasing the strength of the settling field. It is therefore easily seen that the strong fields needed to resolve the fines

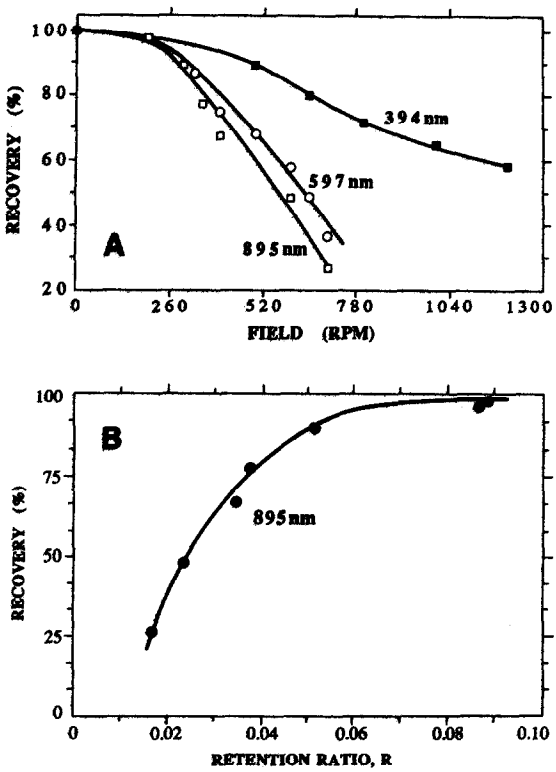

Fig. 4. (A) Sample recovery in SdFFF as function of field strength and particle size. All data represent injections of 4 μl of suspensions containing 1% solids; the flow-rate is constant at 1.0 ml/min. Diameters of the three polystyrene standard particles (Seragen) are indicated in the figure. (B) Sample recovery plotted *vs.* retention ratio, R for the 895-nm standard particle. Experimental conditions are the same as in (A). Significant losses are seen to occur at retentions larger than 25–30 column volumes, corresponding to R values of 0.03–0.04.

in a broadly distributed sample may severely hamper recovery and distort quantification at the high end of the distribution. This effect is clearly illustrated in Fig. 4A, where relative recovery is plotted as a function of field strength for three monodisperse PS latex standards analyzed at different spin rates. The trend of increased sample loss with increasing retention is further demonstrated in Fig. 4B, using the data collected for the largest of the three particles in Fig. 4A. It should be noted that both the metal wall of the channel and the PS beads carry negative charges[21] at neutral pH, which would make this sample less prone to adhesive particle–wall interactions than many other colloidal systems in which the two interact by Van der Waals forces alone or in addition to attractive Coulombic forces. Operation at strong fields must therefore be used judiciously, if quantification of large diameter components is the desired outcome of an FFF analysis.

An alternative way, although more cumbersome than the one presented in Fig. 3, to approach the analysis of broadly distributed samples is to make several consecutive runs at different fields, and only determine size/quantity data for particles of moderate zonal compression; for this purpose, analytically useful retentions appear to range from 5 to *ca.* 30 column volumes. The lower end of this "accuracy window" marks the position in the fractogram where, on the average, transients due to sluggish diffusion seize to play a major role[22] and retentions therefore fairly reflect the diameter of the particle, while the upper end, which is strongly size dependent, is defined by the onset of sample losses of the type shown in Fig. 4B, as well as by other non-ideal behavior discussed below. An example of this strategy, applied to the ten-component sample focused on in the present study, is seen in Fig. 5. Here, three fractograms were collected at constant fields in the "weak", "intermediate", and "strong" range for the

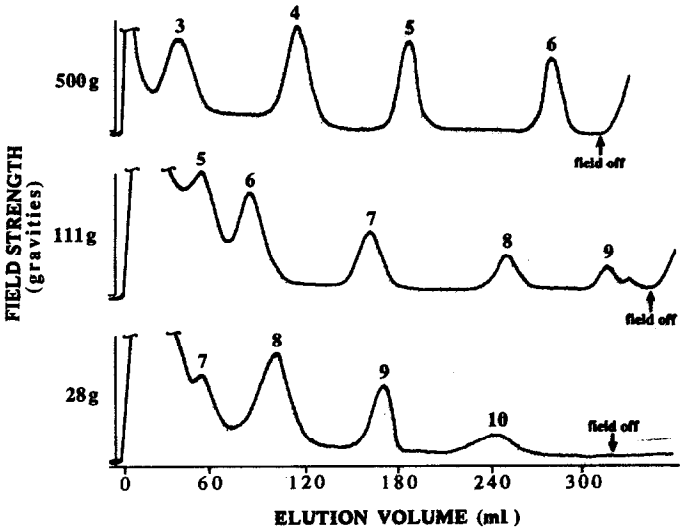

Fig. 5. Sequential SdFFF analyses of the ten-component polystyrene latex sample at constant fields of different strength. The numbers in the fractograms refer to specific components, as defined in Table I. The weak (28 *g*) field analysis was able to visualize component 10, but provided poor resolution of the smaller components. By contrast, the strong (500 *g*) field resolved several of the smaller components, but failed to demonstrate the presence of component 10. The flow-rate was maintained at 2.8 ml/min.

instrument at hand; the flow-rate was kept constant throughout. Each component in the figure is numbered from 1 to 10 in accordance with Table I. The weak field (28 *g*) permitted detection and quantification of component 10, which was otherwise

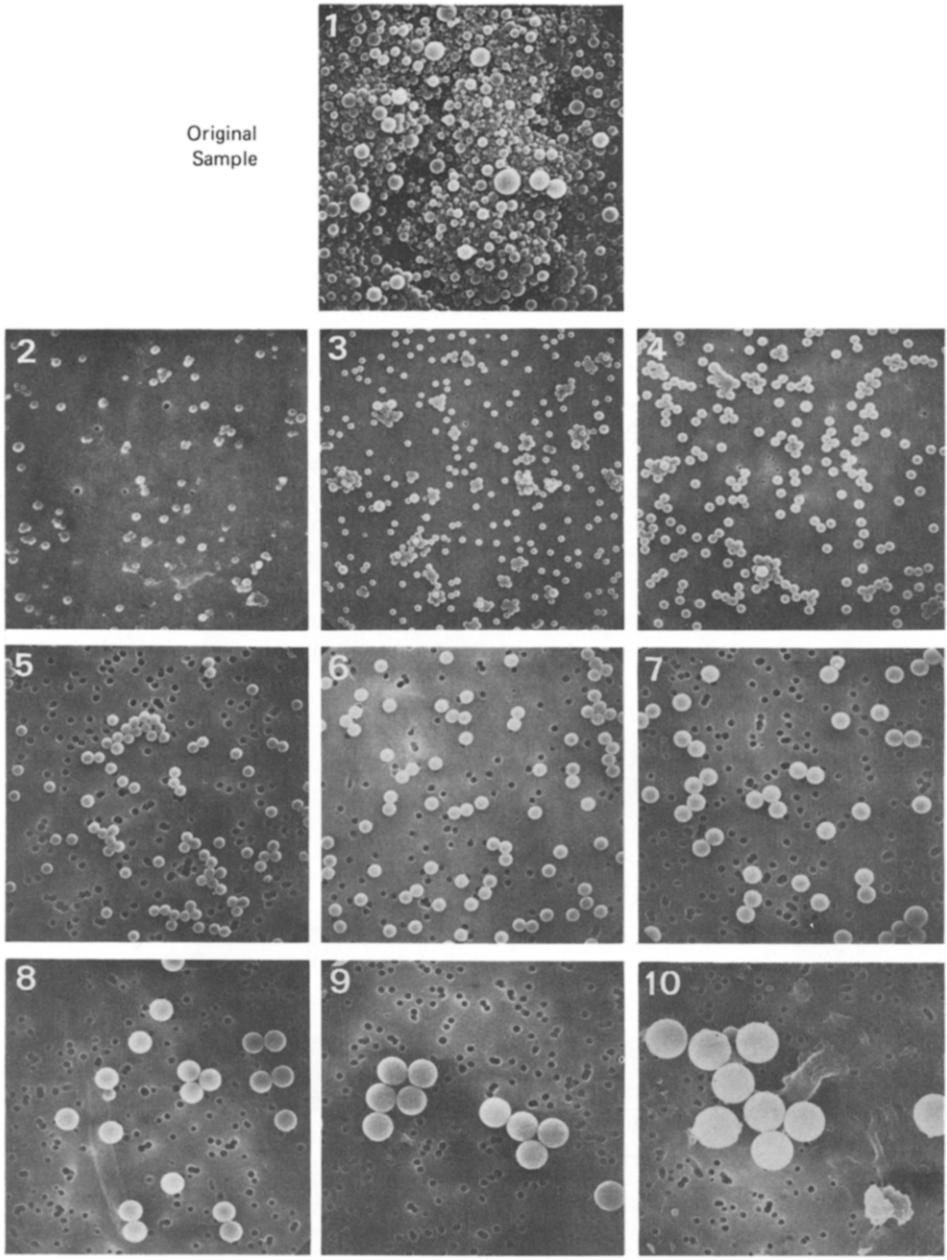

Fig. 6. SEM record of the starting material (top), as well as of the resolved fractions 2 through 10. Sizes measured for the four largest particle types from these micrographs are included in Table I.

undetectable, while this field strength clearly was inadequate for resolution of the finer particles resolved by the stronger fields. During the process, fractions were collected within the "window" for further analysis by SEM (see Table I) and PCS, where the concentration reached above the detection limit for our BI-90 instrument. The SEM images compiled in Fig. 6 give a clear indication that the fractionation is efficient, and produces highly monodisperse cuts without any evidence of contamination from other components in the sample. While the magnification is insufficient to permit accurate sizing of the smaller components, Table I contains SEM size assignments for the four largest particle types separated by SdFFF. These sizes are in good agreement with those determined by AUC.

In addition to affecting sample recovery, as discussed above, the presence of the analytical wall in FFF results in steric exclusion from the interfacial region, as well as in the establishment of a velocity and size dependent lift force directed towards the center of the channel. While the former effect was recognized and modelled by Giddings[13] over a decade ago, the latter is just recently gaining attention, as efforts are under way to expand the range of particle sizes which can be profitably handled by the high resolution SdFFF technique. The present ten-component mixture of monodisper se particles proved to be an ideal sample for demonstrating the existence of such wall effects, as illustrated by Fig. 7. In carrying out the procedure of size analysis at different field strengths described above, it became evident that diameters determined for the larger particles were strongly dependent on the chosen gravitational acceleration G. This obvious anomaly, which was not present for small particles, is an indication that eqn. 9 does not adequately describe the retention of all particles in what is often referred to [9] as the "normal" (as opposed to "steric") mode of FFF operation.

The need for a steric correction to eqn. 9 was realized early on by Giddings and co-workers[13,14], who proposed the modified form of the retention equation listed above as eqn. 10. Further studies by Lee and Giddings[23] supported the notion that parameter γ in this equation had the magnitude of unity, although its actual value was shown to vary with particle size and the chosen experimental conditions. An attempt at re-processing the data in Fig. 7, using eqn. 10 together with values for γ in the range

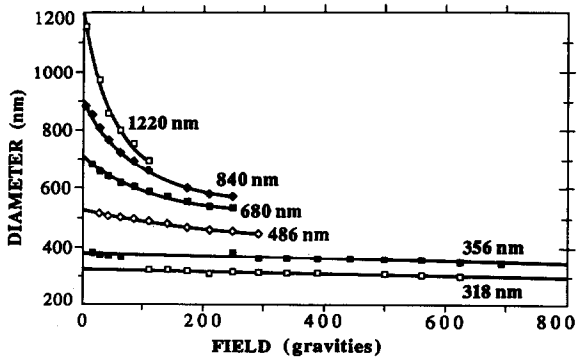

Fig. 7. Effect of field strength on diameters determined by SdFFF using eqn. 9. The small particles behave ideally, and show no effect of G, while a progressively non-ideal behavior is seen for the larger particles. For the four largest particles the diameters listed in Table I were determined by extrapolation to zero field using a fourth order polynomial fit of the data; linear extrapolations were used for the smaller particles. The flow-rate was held constant at 2.8 ml/min.

0.5–2.0, was not successful in removing the influence of field strength on the calculated diameters.

The lack of success in a direct evaluation of particle diameter from retention forced a more detailed analysis of the field effect than first envisioned. Thus, the data set in Fig. 7 is reflecting the sample's behavior under a large number of different field strengths, chosen to allow an extrapolation of diameter data for each particle to a value at zero field, presumably free from wall effects. For the four largest particles, a fourth degree polynomial fit was shown to represent the data with a 99% confidence level, while sizes of the smaller particles were determined by linear extrapolation to zero field. Extrapolated diameters obtained in this way are listed in Table I under the heading "SdFFF-C", and are seen to compare well with those from the AUC over the entire size range. The smallest particle was barely retained even at our maximum field strength of 2000 rpm (692 *g*), and was therefore excluded from this extrapolation procedure.

Also listed in Table I are relative amounts of nine out of the sample's ten components, calculated from areas under the scattering-corrected peaks in the different fractograms. Only baseline resolved peaks with retentions ranging from 5 to 30 column volumes were considered suitable for this analysis, in keeping with the notion of an "accuracy window" mentioned above. Due to its weak retention and poor resolution from the void peak, the smallest particle was not included in this quantification.

Although the relative amounts determined by this approach of multiple runs at different, but constant, field strengths are closer to the true values than those determined by the faster exponential decay method used in the DuPont analysis, they fall short of indicating the actual 10% in relative weight of each component. This is probably due both to difficulties in correctly assessing the position of the baseline when determining the area under a given peak, as well as to the incomplete recovery at high retention illustrated by Fig. 4.

CONCLUSION

One run in the AUC is shown to accurately determine both sizes and relative amounts for complex spherical samples of known density, as in the case of the present ten-component mixture of polystyrene latex particles. Concentration non-idealities are absent in this type of analysis, which involves the observation of freely moving particles, far from any interface and unperturbed by fluid flow. In SdFFF the analysis is complicated by the sample's compression into thin layers at the solid/liquid interface. For small particles at modest retention, the complications are minimal, and good agreement is seen between diameters determined by the SdFFF and AUC techniques. By contrast, particles with diameters above about 500 nm show increasingly severe departures from ideal FFF behavior with increasing field.

For multi-modal samples, such as the one focused on in the present study, diameters can be correctly determined by a systematic observation of values determined at different field strengths, followed by an extrapolation to zero field. This approach is clearly not available for more realistic samples which are often monomodal and highly polydisperse, so that tracking of the field-dependent migration of a particular component becomes impossible. In order to correctly analyze such

samples, it is necessary to develop a modified retention equation which accounts for both the lift forces and steric exclusion effects known to influence the behavior of large particles. Efforts in this regard are currently under way in several laboratories.

The times required for the different approaches were comparable in the cases of AUC and the DuPont SF[3] analysis using an exponentially decaying field. However, unlike in SF[3], the AUC rotor simultaneously accommodates up to seven different samples, which significantly reduces the time per sample. The constant-field approach to SdFFF proposed here is by its very nature time consuming, as it involves multiple runs with relaxation periods of tens of minutes and run times of 1–2 h. It does, however, provide good recoveries of particles in a broad size range, and should be used whenever fractions of exactly sized particles are required.

Despite the wall-related complications discussed above, SdFFF has a clear advantage over AUC in the analysis of samples which require correlations between size and some other sample property, *e.g.* chemical composition or biological activity. Here, one relies on the SdFFF system's proven ability to separate a sample into fractions of uniform size, which can be subjected to one or several secondary analysis steps. To this end, viral infectivity has been associated with fractions representing a given molecular weight[24], X-ray fluorescence in conjunction with SEM has been used to correlate chemical composition with size in an analysis of particulates in stream water[25], and PCS has been used to determine the size associated with particular fractions of samples with unknown density[7]. Although both AUC and SdFFF have been successfully used to analyze samples of unknown density by systematic variations in the density of the carrier or suspension medium[26,27], this approach is only applicable to stable samples that remain unperturbed by changes in the environment. For emulsions and other fragile systems of unknown density it is often appropriate to let SdFFF produce fractions using a highly sample compatible medium, and subsequently size these fractions by an independent method such as PCS or SEM.

ACKNOWLEDGEMENTS

K.D.C. wishes to express her gratitude to Dr. J. Calvin Giddings for many years of educational collaboration. Support for this work via grant number GM 38008-02 from the National Institutes of Health is gratefully acknowledged.

REFERENCES

1 T. Svedberg and H. Rinde, *J. Am. Chem. Soc.*, 46 (1924) 2677.
2 W. Scholten and H. Lange, *Kolloid-Z. Z. Polym.*, 250 (1972) 782.
3 W. Mächtle, *Makromol. Chem.*, 185 (1984) 1025.
4 W. Mächtle, *Angew. Makromol. Chem.*, 162 (1988) 35.
5 J. C. Giddings, *Sep. Sci.*, 1 (1966) 123.
6 F.-S. Yang, K. D. Caldwell, M. N. Myers and J. C. Giddings, *J. Colloid Interface Sci.*, 92 (1983) 81.
7 K. D. Caldwell and J.-M. Li, *J. Colloid Interface Sci.*, 132 (1989) 256.
8 J. C. Giddings, *J. Chem. Ed.*, 50 (1973) 667.
9 M. N. Myers and J. C. Giddings, *Anal. Chem.*, 54 (1982) 2284.
10 K. D. Caldwell, S. L. Brimhall, Y.-S. Gao and J. C. Giddings, *J. Appl. Polymer Sci.*, 36 (1988) 703.
11 J. C. Giddings and K. D. Caldwell, in B. W. Rossiter and J. F. Hamilton (Editors), *Methods in Physical Chemistry*, Vol. 3B, Wiley, 1989, p. 867.
12 J. C. Giddings, F. J. F. Yang and M. N. Myers, *Anal. Chem.*, 46 (1974) 1924.
13 J. C. Giddings, *Sep. Sci. Technol.*, 13 (1978) 241.

14 K. D. Caldwell, T. T. Nguyen, M. N. Myers and J. C. Giddings, *Sep. Sci. Technol.*, 14 (1979) 935.
15 J. C. Giddings, M. N. Myers, K. D. Caldwell and S. R. Fisher, in D. Glick (Editor), *Methods of Biochemical Analysis*, Vol. 26, Wiley, 1980, p. 79.
16 J.-M. Li and K. D. Caldwell, *J. Chromatogr.*, submitted for publication.
17 M. R. Schure, *Anal. Chem.*, 61 (1989) 2735.
18 T. Depireux, F. Dumont and A. Watillon, *J. Colloid Interface Sci.*, 118 (1987) 314.
19 J. C. Giddings and K. D. Calwell, *Anal Chem.*, 56 (1984) 2093.
20 W. W. Yau and J. J. Kirkland, *Sep. Sci. Technol.*, 16 (1981) 577.
21 M. E. Hansen and J. C. Giddings, *Anal. Chem.*, 61 (1989) 811.
22 M. R. Schure, *Anal. Chem.*, 61 (1989) 2735.
23 S. Lee and J. C. Giddings, *Anal. Chem.*, 60 (1988) 2328.
24 K. D. Caldwell, G. Karaiskakis and J. C. Giddings, *J. Chromatogr.*, 215 (1981) 323.
25 G. Karaiskakis, K. A. Graff, K. D. Caldwell and J. C. Giddings, *Int. J. Environ. Anal. Chem.*, 12 (1982) 1.
26 W. Mächtle, *Colloid Polymer Sci.*, 262 (1984) 270.
27 J. C. Giddings, G. Karaiskakis and K. D. Caldwell, *Sep. Sci. Technol.*, 16 (1981) 607.